EXTRAPOLATING POWER-RAMP PERFORMANCE CRITERIA FOR CURRENT AND ADVANCED CANDU® FUELS†

M. TAYAL and G.G. CHASSIE

Atomic Energy of Canada Limited
Fuel Design Branch
2251 Speakman Drive
Mississauga, Ontario
Canada L5K 1B2

ABSTRACT

To improve the precision and accuracy of power-ramp performance criteria for high-burnup fuel, we have examined in-reactor fuel performance data as well as out-reactor test data. The data are consistent with some of the concepts used in the current formulations for defining fuel failure thresholds, such as size of power-ramp and extent of burnup.

Our review indicates that there is a need to modify some other aspects of the current formulations; therefore, a modified formulation is presented in this paper. The improvements mainly concern corrodent concentration and its relationships with threshold stress for failure. The new formulation is consistent with known and expected trends such as strength of Zircaloy in corrosive environment, timing of the release of fission products to the pellet-to-sheath gap, CANLUB coating, and fuel burnup.

Because of the increased precision and accuracy, the new formulation is better able to identify operational regimes that are at risk of power-ramp failures; this predictive ability provides enhanced protection to fuel against power-ramp defects. At the same time, by removing unnecessary conservatisms in other areas, the new formulation permits a greater range of defect-free operational envelope as well as larger operating margins in regions that are, in fact, not prone to power-ramp failures.

® CANDU is a registered trademark of Atomic Energy of Canada Limited (AECL).

† Presented at the 21st Annual Conference of Canadian Nuclear Society, Toronto, Ontario, 2000 June 11-14.

1. INTRODUCTION

The current defect thresholds for fuel failures caused by power-ramps were developed empirically from irradiation data. They have been used for design assessments and to devise fuelling schemes to avoid power-ramp failures. To-date, the performance of CANDU fuel has been excellent.

In some advanced fuel cycles involving slightly enriched uranium (SEU), core-wide fuel burnups will be considerably higher than in the current natural-uranium (NU) cores. This change requires an extrapolation of power-ramp defect thresholds in the high-burnup regions where the performance data and operating experience are limited. Programs are currently underway at Atomic Energy of Canada Limited (AECL) to achieve this objective. This paper describes a step in that direction.

The specific objectives of this paper are to examine the consistency of relevant failure criteria and methodology using available data, and to develop an approach for extrapolating the current power-ramp performance criteria to advanced fuel cycles. The scope includes power-ramp performance at circumferential ridges (pellet-to-pellet junctions) for the full range of powers and power-ramps that are relevant to normal operating conditions of CANDU fuel. The main focus is on simple idealized power histories, consisting of a constant pre-ramp power followed by a power-ramp.

2. BACKGROUND

The literature reports two mechanisms for power-ramp failures at circumferential ridges: (1) stress-corrosion cracking (SCC) [1, 2] and (2) mechanical overstrain of Zircaloy [1, 3] . Failures of the second type have been comparatively much less numerous than those of the first type. The scope of this paper covers both possibilities of sheath failure.

In Zircaloy-clad UO_2 fuel, the primary driving force for power-ramp failure at the circumferential ridge is pellet expansion, which in turn leads to stresses and strains in the sheath. The mechanical energy required for sheath failure depends on the availability and concentration of fission-product corrodents (such as iodine) and on the strength of Zircaloy to resist the stresses and strains under the corrosive environment. The latter depends on burnup. Therefore, the defect threshold is dependent on the full power history, the transient powers during refuelling, and the detailed internal design of the fuel.

The approach used in the current power-ramp failure curves—Fuelograms—was first developed in mid-1970s through a statistical examination of non-CANLUB data. This review identified the major parameters of importance and their trends. Then, when CANLUB data became available at a later date, the major parameters and trends determined from non-CANLUB data were retained, but their absolute levels were adjusted to reflect the effects of CANLUB.

In the current approach, the ramped power is used as a measure of corrodent concentration, and power-ramp as a measure of mechanical energy imparted on the sheath. Each of the two parameters is considered to have an independent threshold for failure as a function of burnup. For power-ramp failure to occur, the threshold values of both parameters need to be exceeded independently; the failure threshold of one is not related to the failure threshold of the other. Thus the threshold value for failure from each effect is considered to be a separate and independent function of burnup and CANLUB.

After the preceding approach had been established, a large amount of new information became available through additional power-reactor operating experience, research-reactor tests, and out-reactor tests. We reviewed this information, to gain further insights into the operating mechanisms and to establish trends among the major parameters. These characteristics were then compared with assumptions and relationships contained in the available correlations for power-ramp defect thresholds, for example References 1 and 4.

We begin by discussing two key observations from the review; these led to a revised formulation for power-ramp defect criteria.

3. OBSERVATION # 1: STRENGTH OF ZIRCALOY

Over the last quarter-century, many " materials science" tests were performed worldwide on the strength of Zircaloy; see, for example References 5 to 8. These tests describe how the strength of Zircaloy is influenced by the combined actions of mechanical energy (i.e., stress and strain), corrodent concentration (e.g., iodine, cesium, cadmium, etc., and their combinations), and neutron damage.

Figure 1 shows illustrative examples of the results of "materials science" tests. The data of Peehs et. al. [5] in Figure 1(a) show that very low levels of corrodent concentration (iodine) have no significant impact on strength of Zircaloy. As the corrodent concentration (iodine) increases beyond a certain level, the microstructure of Zircaloy weakens rapidly, and it fails at a progressively smaller amount of mechanical energy. The effect of corrodents eventually saturates out, and Zircaloy retains some strength even at relatively high levels of corrodents. Thus the threshold stress (i.e., power-ramp) for failure is a strong, continuous and smooth function of the corrodent concentration (i.e., power level); the two are not independent.

Figure 1(a) also shows that at any given level of iodine there is always some level of mechanical energy that will fail Zircaloy. Thus there does not exist a cut-off level of iodine below which Zircaloy cannot fail given sufficient mechanical energy. At levels when iodine does start to have an effect on strain-to-failure, the effect is gradual. These observations mean that there is no threshold power level (corrodent concentration) below which sheath failure can be precluded regardless of the magnitude of the power-ramp (mechanical energy).

The data of Lunde and Videm [6] in Figure 1(b) show that the strength of Zircaloy generally decreases with burnup. From the data of Lunde and Videm, one can also obtain independent qualitative support for the trends exhibited by the data of Peehs, by looking at what happens at constant burnup for the two tested levels of iodine. For example, line AB represents a fast neutron dose of 2×10^{21} neutrons/cm^2. At the lower level of iodine, 5 mg, the failure stress ranges between points 3 and 4; thus the "threshold" for failure at this burnup and iodine level is at point number 3—which is about 400 MPa. Similarly, at the higher level of iodine—20 to 250 mg—the failure threshold is about 130 MPa. Thus at a constant burnup, Lunde and Videm's data show that the failure threshold stress decreases significantly with increasing levels of corrodent. This trend agrees with the message contained in the data of Peehs et. al.

It is easy to visualize from Figure 1(b) that had the tests also been done at other intermediate levels of iodine, intermediate values of threshold stresses would have been obtained. Thus at any given burnup, there is not one combination of threshold iodine and threshold stress that causes failure. Rather, many such combinations exist. This is also consistent with the message from the data of Peehs et. al (Figure 1(a)).

Many experiments of the above type have been reported in the literature; see, for example, the bibliographies in References 7 and 8 . Figure 1(c) illustrates the conclusion that we have drawn pertinent to this paper. The figure shows how various levels of corrodents affect the strength of Zircaloy at any given burnup. The points labelled 1 to 4 on Figure 1(c) are derived from similarly labelled points in Figure 1(b).

Figure 1(c) merely summarizes the theme discussed earlier: At extremely low levels of corrodent, the corrodent has no significant effect on the strength of Zircaloy. At moderate levels, the corrodent starts to reduce the strength of Zircaloy, but this effect saturates beyond a sufficiently high level of corrodent concentration. In this paper, the shape that is created by this effect is called an "inverted-S" shape.

The effect of CANLUB is to reduce the corrodent concentration at the sheath surface. Alternately, in terms of power levels, the net effect of CANLUB is to move the inverted-S curve of Figure 1(c) to the right.

Burnup has a number of direct and indirect influences on sheath integrity. First, burnup monotonically increases irradiation damage, which is proportional to peak sheath stress attainable, which is inversely proportional to resistance to failure. This would tend to move the inverted-S curve downward. Second, fast neutrons damage the microstructure of Zircaloy, which reduces its strength to resist stresses. This mechanism also tends to move the inverted-S curve downwards. Third, higher burnup is generally associated with increased levels of oxides and hydrides on the sheath surface. This trend, too, reduces sheath strength and moves the inverted-S curve downwards. Fourth, burnup increases the total inventory of fission products that are produced. This phenomenon increases the absolute amount of fission products that are available in the pellet-to-sheath gap, for a given percentage gas release. Hence burnup increases the corrodent concentration plotted on the "x"-axis. This mechanism tends to move the curve towards the left. Fifth, burnup influences pellet and sheath diameters, stresses and strains through a variety of other processes such as densification, fission-product swelling, sheath creep, pellet temperature, etc. In summary, both axes of Figure 1(c) are affected by burnup, and burnup can influence the location as well as the angle of the inverted-S curve.

In short, the threshold stress for failure of Zircaloy is a continuous and smooth function of the corrodent level and of burnup. Moreover, there is no cut-off limit of corrodent concentration below which Zircaloy is immune to failure, regardless of the amount of mechanical energy imparted on Zircaloy.

4. OBSERVATION # 2: FISSION-PRODUCT RELEASE

Figure 2 shows typical measurements of fission-gas pressure, taken on-power during an instrumented experiment in a research reactor [References 9, 10]. It shows that there is a time-delay between production of fission gas and its eventual release to the pellet-to-sheath gap [9,10]. The following paragraphs explain the reason for the time-delay [9,10].

Fission-gas release within a fuel element is a very complex process and has already been explained in many papers. An overview is given in Reference 10. The fission-product inventory within the fuel sheath is determined primarily by the fuel operating temperature (i.e., power) and its duration (i.e., burnup). There are many other contributing factors as well; please see Reference 10 for a more detailed discussion.

Fission continuously produces fission gases inside the grains of UO_2. The gas then diffuses to grain boundaries because of its concentration gradients within the grains. After diffusion, the fission gas collects in bubbles at the boundaries of the grains of UO_2. The bubbles have a given capacity to store the gas. With continued operation at power, the amount of fission gas at the grain boundaries eventually exceeds the capacity of the bubbles to store it. At first, the excess gas is accommodated by overpressure in the bubbles. A subsequent change in power creates micro-cracks in UO_2, thereby providing a path for the fission gas to escape from the bubbles. This eventually releases the excess gas to the pellet-to-sheath gap. In short, gas diffuses to the grain boundaries *during* operation at a given power, and is then released to the pellet-to-sheath gap during the *next* change in power. In between, the bubbles on grain boundaries act as “holding tanks” for the gas.

This means that the amount of fission products that is available to assist in the power-ramp failure of the sheath is the amount that has diffused during operation at the pre-ramp power. The additional fission products, which diffuse during operation at the ramped power, contribute significantly to post-irradiation measurements, but these additional fission products are not available at the surface of the sheath when power-ramp damage occurs.

5. PROPOSED FORMULATION

The review confirmed the validity of some of the operational parameters used in the current power-ramp defect thresholds, such as use of power-change as an indicator of incremental stress and strain on the sheath during the power-ramp [11]. The results also showed that use of some other parameters needs to be improved, particularly in the areas of determining the corrodent concentrations and detailed stresses during the power-ramp, and their effects on power-ramp defects. Using these results, we established a revised analytical approach—summarized below—that lays out a path for establishing modified criteria for power-ramp performance of CANDU fuel.

- Similar to the current approach, the new approach considers power-change a valid measure of pertinent stress and strain in the sheath.

- Likewise, burnup is an appropriate measure of a variety of influences pertinent to power-ramp failures, as discussed earlier.

Some features of the new approach do differ considerably from the current approach in the following ways:

- There is a strong link between the corrodent concentration and the allowable value of stress. Lower levels of corrodents permit higher levels of stress without causing fuel failures. Thus the defect thresholds for stress and for corrodent are not independent of each other but are linked through a continuous and smooth relationship.
- If the stress is high enough, Zircaloy can fail at any level of corrodent concentration — even zero [12]. Therefore the new approach does not require that a minimum concentration of corrodents (i.e. power) is necessary for power-ramp failures. Rather, the stress (power-ramp) required for sheath failure is treated as a function of corrodent concentration (power level) and sheath strength (burnup).
- For simple power-histories—constant power followed by a single ramp—pre-ramp power (rather than ramped power) is a better indicator of corrodent concentration at the sheath surface during the ramp.
- Comparatively fewer irradiation data are available for more complex power histories such as extended burnups, multiple ramps, and declining pre-ramp powers. For these situations, the available data and the derived thresholds need to be supplemented by a mechanistic treatment using fundamental parameters such as sheath stress and fission-gas release.
- The above mechanistic approach is also required for extrapolating the power-ramp defect threshold curves to new operating conditions such as higher coolant temperatures and higher coolant pressures. Likewise, the mechanistic approach is required to extrapolate the power-ramp defect thresholds to different design configurations such as sheaths of different thicknesses, changed pellet geometry, and altered pellet–sheath clearances, etc.

Next, we describe how the above formulation was verified and which data-base was used for the verification.

6. POWER-RAMP DATA

To confirm the viability of the identified operational parameters and formulation in defining power-ramp performance, we have checked how well the various operational parameters exhibit the expected trends.

In this part of the investigation, we are looking for trends rather than absolute magnitudes; hence it does not matter whether the tested region is from CANLUB or non-CANLUB fuel. The more important considerations are the density of defects and their operational ranges.

In-reactor data are available from commercial power reactors and from experimental irradiations conducted at the Chalk River Laboratories (CRL) of AECL. Sometimes, by design, CRL irradiations tend to contain experimental variables that might influence the defect thresholds. One example is pellets with circumferential and longitudinal grooves, which were investigated as potential sites to store fission gases. Another example is chamfers with deeper angles, which were also investigated as a potential site for storing fission gases. Both these changes increase pellet temperatures and influence fission gas release and pellet expansion. Such phenomena could potentially introduce some trends in this data that are dissimilar from the power-reactor data. Hence at this time we have not considered the experimental data in establishing trends, until suitable correction factors can be applied as appropriate to account for the effect of experimental variables in each experiment.

Our current database of power-ramps consists of 894 ramps with 184 defects, covering a burnup range of 0 to 800 MW•h/kg U in CANLUB and non-CANLUB fuels. For the fairest possible test of the new hypothesis, we looked for a defect-dense region in a narrow burnup range, with wide ranges and combinations of powers and power-ramps in the failed fuel.

The above search criteria were best met by non-CANLUB fuel in the burnup range of 140 ± 20 MW•h/kg U. The second most-densely populated region in our data-base consists of defects in CANLUB fuel at 200 ± 20 MW•h/kgU. The above two regions together include 186 power-ramps and contain 56 defects at circumferential ridges, in the two relatively narrow zones of burnups.

By comparing the defects within and among the above 2 regions, we could deduce trends exhibited by the new and current approaches with respect to power, power-ramp, burnup, and CANLUB. These are discussed in the following paragraphs.

7. TRENDS

We know from "materials science" tests shown in Figure 1 that, at any given burnup, the mechanical energy (power-ramp) for failure and the corrodent concentration (power level) are related by an inverse-S curve. The new and current approaches use pre-ramp power and ramped power, respectively, to represent the corrodent concentration. We checked whether these two representations of corrodent concentration match the expected inverse-S shape for failure of Zircaloy. For this reason, we plotted the change in power—to represent mechanical energy—as a function of two different representations of corrodent concentration: (1) pre-ramp power to represent corrodent concentration, and (2) ramped power to represent corrodent concentration. This was done for the most data-rich region in our database, i.e., at 140 MW•h/kg U in non-CANLUB fuel.

The results for the two representations of corrodent concentration are shown in Figures 3a and 3b respectively. With the new approach, the in-reactor data are quite consistent with the inverted-S shape expected from the independent "materials science" information in Figure 1. Also, the new approach provides a much sharper demarcation between defective and intact fuels. These observations confirm that pre-ramp power is indeed a better descriptor of corrodent concentration for power-ramp failures, as is also suggested by the independent tests discussed under "Observation # 2".

Figure 4(a) shows the thick CANLUB data at 140 MW•h/kg U and compares them to corresponding non-CANLUB data. The figure shows that the new approach captures the expected trend regarding the effect of CANLUB; that is, CANLUB moves the defect threshold to the right—as expected and discussed earlier.

The defect threshold shown in Figure 4(a) for CANLUB fuel was derived from the established data-base. We compare the defect threshold to some operating experience of the Bruce-A station and a CANDU-6 station. Refuelling shifts in these reactors do not result in power-ramp failures. Previous studies have identified that the highest risk of power-ramp failures is encountered during 4-bundle shifts in the Bruce-A reactor operating at 100% power. Figure 4(a) compares the high-burnup end of this data (at about 130 MW•h/kg U) with the new defect threshold. The Bruce-A data for intact fuel do lie below the defect threshold. This confirms that the defect threshold is also consistent with operational experience in the Bruce-A and CANDU 6 stations.

Figure 4(b) shows that the new approach also captures the expected trend with respect to burnup; that is, burnup decreases the defect threshold.

Figure 5 compares the three defect threshold curves, derived above, using the new approach for non-CANLUB fuel at 140 MW•h/kg U, thick CANLUB fuel at 140 MW•h/kg U, and thick CANLUB fuel at 200 MW•h/kg U. The major trends are summarized as follows: At any given burnup, there exist many interlinked combinations (not just one) of threshold power-ramps and powers at which fuel failures can begin; the relationship between the two is consistent with the "inverted-S" shape expected from independent "material science" tests; the defect threshold decreases with burnup; and

CANLUB increases the defect threshold. All these trends are consistent with expectations.

Figure 6 shows that the scatter—defined as the region that simultaneously contains failed and intact fuels—is 5 kW/m in the new approach. This scatter is lower than in the current approach [1].

8. IMPACT

We checked whether the new formulation differs from the current approach in identifying operational regimes that protect the fuel from power-ramp failures. Figure 7 shows the 29 power-ramp defects in non-CANLUB fuel at 140 ± 20 MW•h/kgU. The figure also shows the pertinent Fuelogram defect threshold for non-CANLUB fuel, as well as a new threshold from the proposed new approach. Compared to Fuelograms, the new approach identifies different defect thresholds in the hatched and cross-hatched regions.

The hatched region of Figure 7 relates mainly to refuelling ramps in non-CANLUB fuel. Even though Fuelograms flag this zone as being a risky region, it contains no defected bundles and many intact bundles (the latter—i.e., the intacts—are not shown in Figure 7 to reduce clutter and improve clarity). To reflect this, the new approach does identify this region as one which is not at risk of power-ramp failures. For any given initial power in the hatched region, the new defect thresholds would permit power-ramps that are generally about twice as high as those permitted by Fuelograms. Thus the new defect thresholds significantly extend the operational regime within the hatched region which is not at risk of power-ramp failures.

As noted earlier, the above review is based mainly on non-CANLUB fuel. This choice was necessitated by the significantly lower incidence of fuel failures in CANLUB fuel; but we do expect the new methodology to have qualitatively similar relative effects on the defect thresholds of CANLUB fuel as well.

9. SYNERGY

To extend power-ramp defect thresholds to higher burnups, one aspect of our intended strategy is to take advantage of synergy that accrues from treating data at a mechanistic level. Specifically, there is a benefit in being able to derive trends from data-rich regions of one type of fuel, and applying them to data-sparse regions of other types of fuel such as high-burnup SEU fuel. To be able to do that, one needs to be able to collapse all relevant data into one family. We checked whether the proposed approach would achieve this reduction in conjunction with appropriate mechanistic parameters.

To do that, we need to "translate" operational, design and manufacturing information—such as powers, power-ramps, clearances, density, etc.—into mechanistic information such as mechanical energy, corrodent concentration, local strength, etc.

References [13] and [14] outline an approach for achieving that, and provide a detailed description. A brief summary is given below for completeness.

The computer codes ELESTRES [15], SHEATH, FEAST [16], and INTEGRITY [14] provide a significant head start in the above direction. ELESTRES translates the power history and design information into fission-product concentration and local deformations of the pellet and the sheath at the circumferential ridge. The FEAST code translates the pellet and sheath deformations into strain energy imparted on the sheath. At the same time, the FEAST code also accounts for local bending of the sheath near the circumferential ridge and the resulting multiaxial stresses and strains. The INTEGRITY code uses Lunde and Videm's measurements of the effect of neutron damage on the mechanical energy required to fail Zircaloy (Figure 1b). This energy is used in conjunction with FEAST results to calculate a strain energy ratio, which is a relative measure of the amount of imparted mechanical energy as a ratio of that required to fail Zircaloy at that burnup for a given concentration of fission products.

Previous studies have already demonstrated that the mechanistically-based approach is able to account for the following effects:

- Full power history, including preconditioning and effects of declining power history
- Effects of axial variations in power and consequent axial mixing of fission products
- Changes in element diameter [13,14,]
- Changes in internal design

We now investigated whether the mechanistic parameters, in conjunction with the proposed new approach, are able to collapse the data at various burnups into one family. For this reason, the above codes were used to calculate the mechanistic parameters for each power-ramp in the two burnup-ranges mentioned earlier. It is recognized that the current versions of the preceding computer codes need some evolutions to be fully effective for the purpose of establishing power-ramp failure thresholds under all conditions expected in a SEU core. Nevertheless, we used the current versions of the codes to obtain an initial indication of the viability of the intended approach.

At the mechanistic level, these computer codes use an approach that automatically covers the effects of burnup on fission-gas release, pellet deformations, sheath stresses and strains, and sheath strength. Thus the effects of burnup are already reflected in the 2 axes used in the mechanistic curve of Figure 8. Hence, at the mechanistic level, we do not expect to see any difference in the thick CANLUB data at the two tested burnups. This expectation is indeed confirmed by Figure 8: The two burnup-groups of failed fuel and intact fuel automatically form one family on the mechanistic plots. This observation confirms that the methodology has a good prospect of being able to collapse the data for all the various burnups into one generic curve of defect threshold.

Another advantage of a "universal" failure criterion would be to account for possible variations in the amount of CANLUB as a function of burnup—if that effect is confirmed and is deemed appropriate for consideration in power-ramp performance. An exploratory study has already demonstrated that this influence can be captured successfully by the computer codes, if required. The same study has also demonstrated that this approach can also be used to quantify the benefit of designing fuel with thicker layers of CANLUB should it become desirable to do so for any of the advanced cycles.

10. SUMMARY AND CONCLUSIONS

In summary, the new formulation recommends the following changes from the current approach:

- The pre-ramp power should be used as the measure of corrodent concentration.
- At any given burnup, the mechanical energy (power-ramp) for failure is a continuos and smooth function of the corrodent concentration (pre-ramp power). This means that at any given burnup, many combinations of powers and power-ramps define fuel failure thresholds—not just one combination.
- There is no threshold level of corrodent concentration (power) below which the sheath is immune to failure, regardless of the size of the mechanical energy (power-ramp).

Illustrative applications of the new formulation have shown a number of advantages: the new formulation is consistent with all known and expected trends with respect to the effect of corrodent level on the strength of Zircaloy; the timing of fission-product release to the pellet-to-sheath gap; CANLUB coating; and fuel burnup. The new formulation provides a sharper demarcation between defective and intact fuels; and its scatter of about 5 kW/m is lower than that of the current approach. Illustrative defect thresholds from the new approach are also consistent with successful experiences during 4-bundle shifts in the Bruce-A reactor at 100% power, and with CANDU 6 station experience.

Moreover, different sets of data collapse into one "family" when computer codes and mechanistic parameters are used to define the fuel defect thresholds. This reduction provides a basis for significant synergy, in that we can derive trends from data-rich regions of one type of fuel, and extrapolate them to data-sparse regions of other types of fuel such as high-burnup SEU fuel.

The new formulation significantly improves the precision and accuracy in defining power-ramp defect thresholds. As a consequence, the new formulation is better able to identify regions that are at risk of power-ramp failures; this predictive capability provides enhanced protection to the fuel against power-ramp defects. By removing unnecessary conservatisms, the new formulation permits a larger operational envelope as well as higher operating margins in regions that are, in fact, not at risk of power-ramp failures.

11. ACKNOWLEDGEMENTS

The authors gratefully acknowledge valuable discussions and suggestions from A.M. Manzer, P.K. Chan, J.H.K. Lau, P. Boczar, M. Floyd, and J. Sullivan.

12. REFERENCES

[1] W.J. Penn, R.K. Lo, J.C. Wood, "CANDU Fuel — Power Ramp Performance Criteria", Nuclear Technology, Vol. 34, July 1977, 249-268.

[2] M.R. Floyd, R.J. Chenier, D.A. Leach, R.R. Elder "An Overview of the Examination of Fuel as Follow-up to the 1988 November Overpower Transient in Pickering NGS-A Unit 1", Third International Conference on CANDU Fuel, Canadian Nuclear Society, 1992 October 4-8, Chalk River, Canada.

[3] H. Sakurai, Y. Wakashima, K. Ito, M. Sasaki, T. Nomata, Y. Tsukuda, H. Hayashi, D. Kubota, "Irradiation Characteristics of High Burnup BWR Fuels", International Topical Meeting on Light Water Reactor Fuel Performance, American Nuclear Society, Park City, U.S.A., 2000 April 10-13.

[4] R. da Silva, "CAFE - A Probabilistic Model for Predicting CANDU Fuel SCC", Third International Conference on CANDU Fuel, 1992 October 4-8, Chalk River, Canada.

[5] M. Peehs, H. Stehle, E. Steinberg, "Out-of-Pile Testing of Iodine Stress Corrosion Cracking in Zircaloy Tubing in Relation to the Pellet-Cladding Interaction Phenomenon", Zirconium in the Nuclear Industry, (Fourth Conference), ASTM STP 681, 1979, 244-260.

[6] L. Lunde, K. Videm, "The Influence of Testing Conditions and Irradiations on the Stress Corrosion Cracking Susceptibility of Zircaloy", Journal of Nuclear Materials, Vol. 95, 1980, 210-218.

[7] B. Cox, J.C. Wood, "Iodine Induced Cracking of Zircaloy Fuel Cladding — A Review", Atomic Energy of Canada limited Report, AECL-4936.

[8] B. Cox, "Pellet-Clad Interaction (PCI) Failures of Zirconium Alloy Fuel Cladding — A Review", Journal of Nuclear Materials, Vol. 172, 1990, 249-292.

[9] F.R. Campbell, R. Deshaies, M.J.F. Notley, "Transient Fission Gas Releases Within UO_2 Fuel Elements Following Power Increases", Atomic Energy of Canada Limited Report, AECL-4912, 1974.

[10] M.J.F. Notley, I.J. Hastings, "A Microstructure-Dependent Model For Fission Product Gas Release And Swelling in UO_2 Fuel", Nuclear Engineering and Design, Vol. 56, 1980, 163-175.

[11] P.J. Fehrenbach, I.J. Hastings, P.A. Morel, R.D. Sage, A.D. Smith, "Dimensional Response of CANDU Fuel to Power Changes", Atomic Energy of Canada Limited Report, AECL-7837, 1982.

[12] D.G. Hardy, "The Effect of Neutron Irradiation on the Mechanical Properties of Zirconium Alloy Fuel Cladding in Uniaxial and Biaxial Tests", Irradiation Effects on Structural Alloys for Nuclear Reactor Applications, American Society for Testing and Materials, ASTM STP 484, 1970, 215-258.

[13] M. Tayal, E. Millen, R. Sejnoha, G. Valli, "A Semi-Mechanistic Approach to Calculate the Probability of Fuel Defects", Third International Conference on CANDU Fuel, Canadian Nuclear Society, Pembroke, 1992. Also, Atomic Energy of Canada Limited Report, AECL-10642.

[14] M. Tayal, K.D. Hallgrimson, J.R. McQuarrie, P. Alavi, S. Sato, Y. Kinoshita, T. Nishimura, "INTEGRITY: A Semi-Mechanistic Model for Stress Corrosion Cracking of Fuel", IAEA Technical Committee Meeting on Water Reactor Fuel Element Modelling at High Burnup and Its Experimental Support, Windermere, U.K., 1994.

[15] M. Tayal, "Modelling CANDU Fuel Under Normal Operating Conditions: ELESTRES Code Description", Atomic Energy of Canada Limited Report, AECL-9331, 1987.

[16] M. Tayal, "FEAST: A Two-Dimensional Non-Linear Finite Element Code for Calculating Stresses", Seventh Annual Conference of Canadian Nuclear Society, Toronto, Ontario, Canada, 1986 June 8-11.

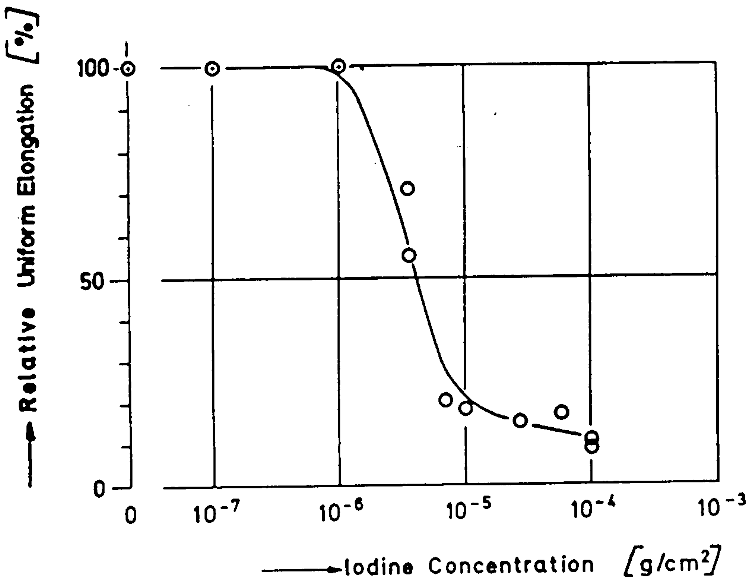

(a) Strength of Unirradiated Zircaloy (Peehs et. al)

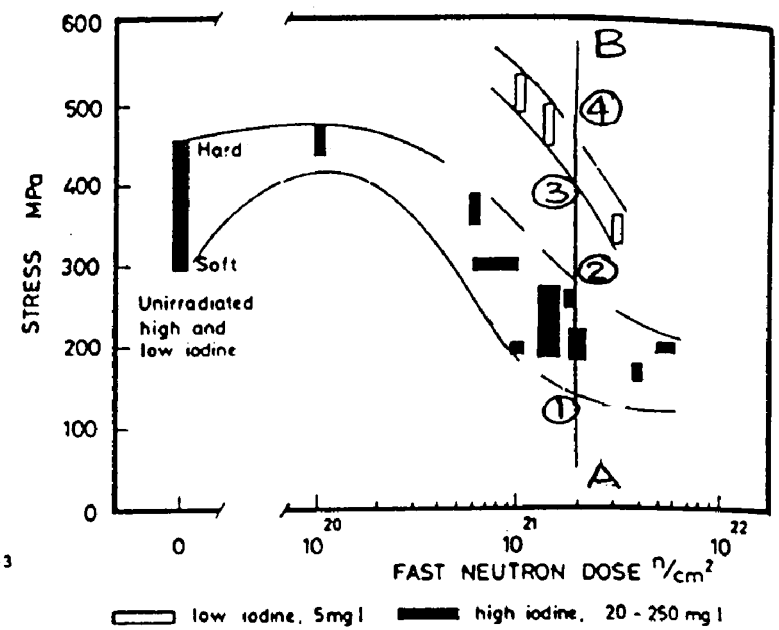

(b) Strength of Irradiated Zircaloy (Lunde and Videm)

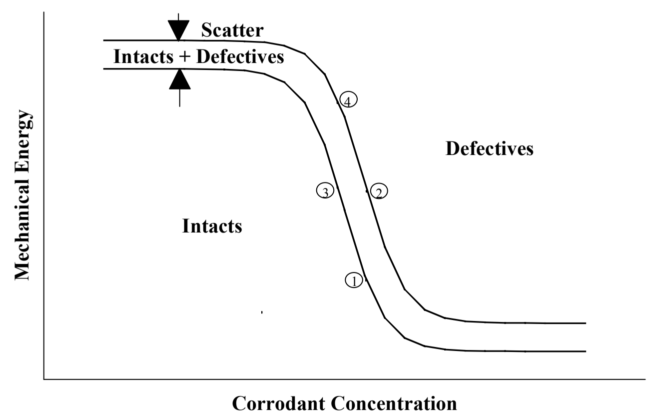

(c) Generic Shape of Defect Threshold at a Given Burnup for a Constant Hold Period

Figure 1 Effects of Corrodents and Irradiation on the Strength of Zircaloy

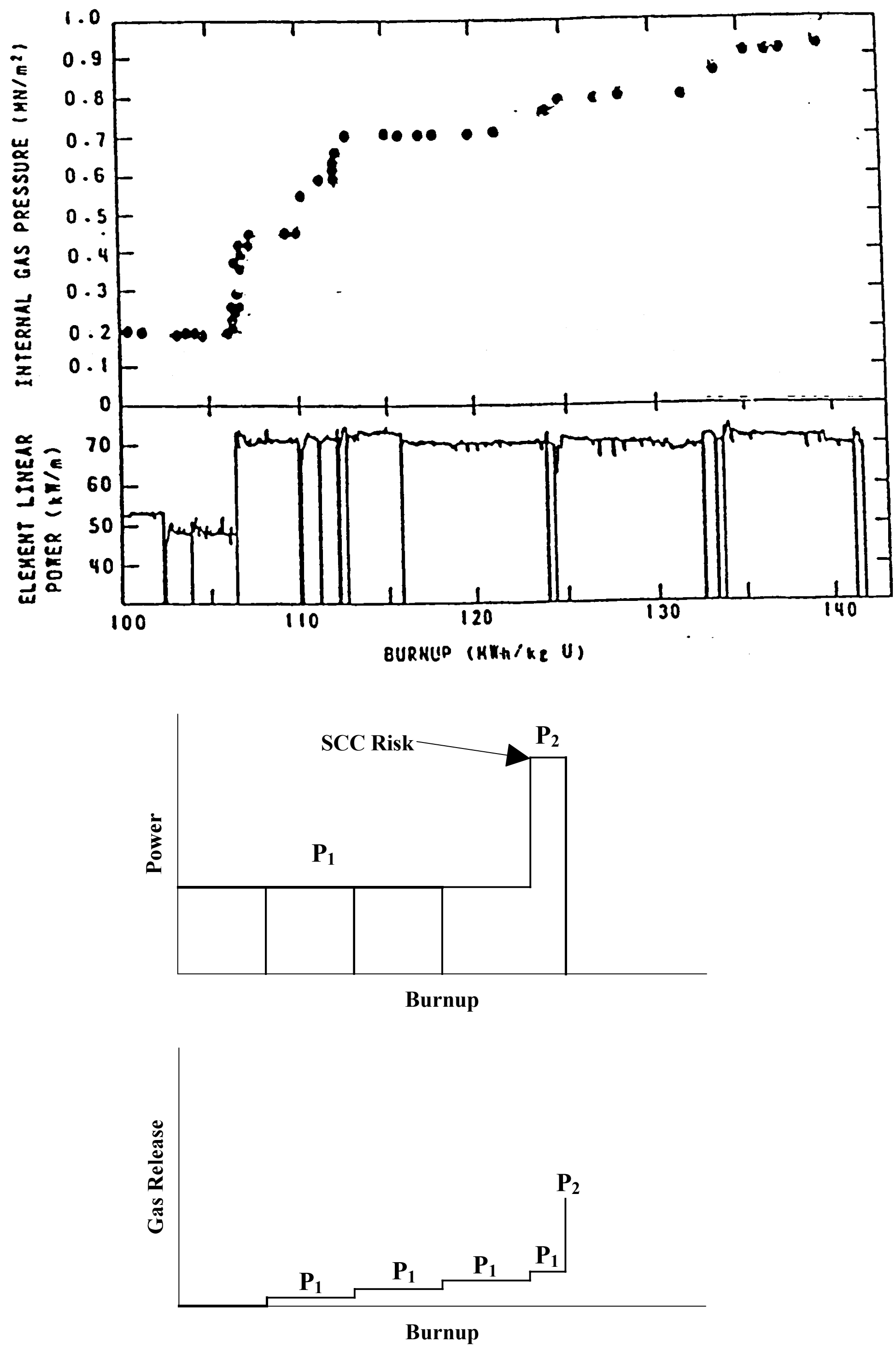

Figure 2 **Time-delay in Fission-gas Release**

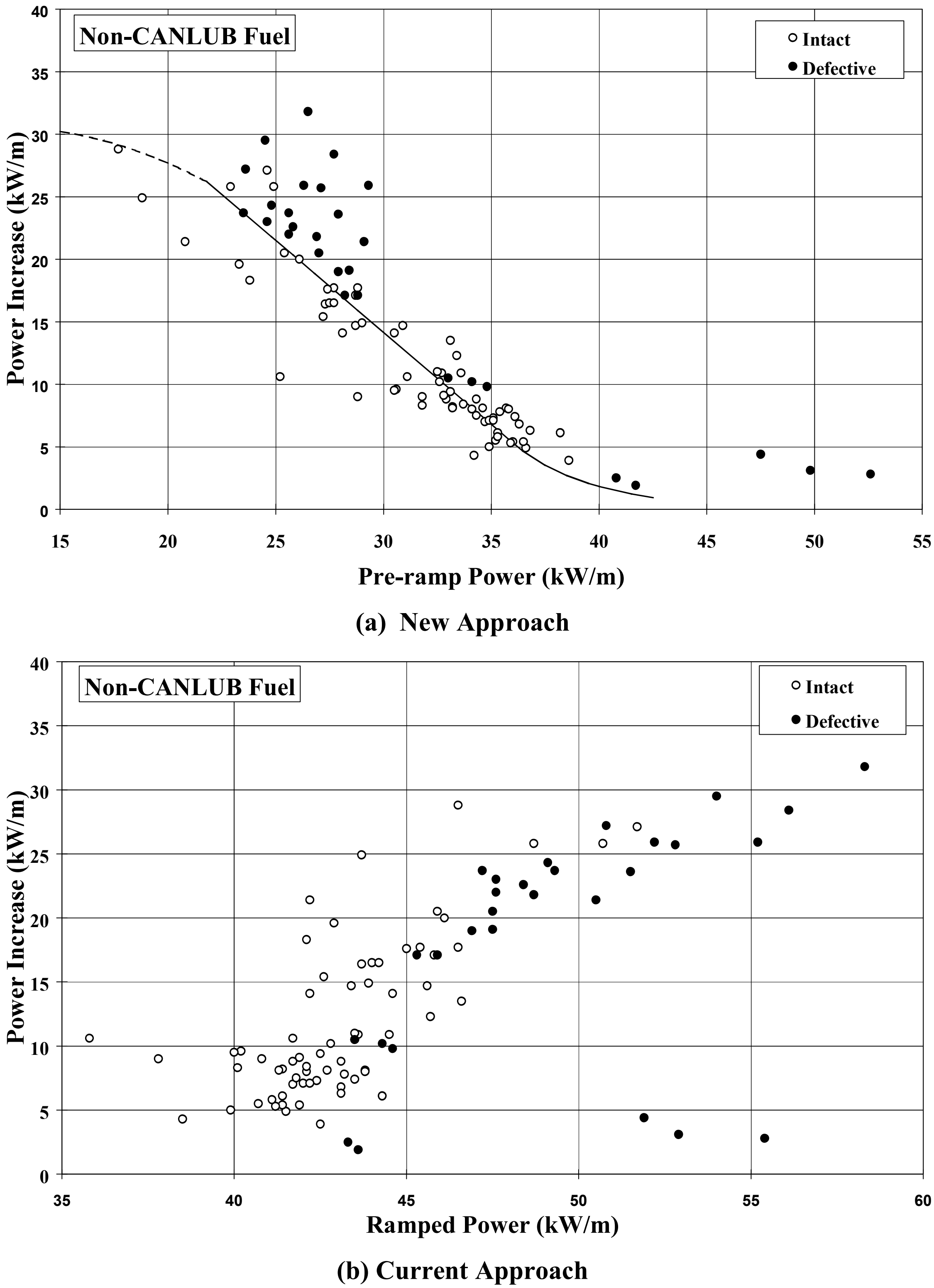

Figure 3 Shape of Failure Conditions from Actual Experience: Non-CANLUB Power Reactor Fuel at 140 ± 20 MW·h/kgU

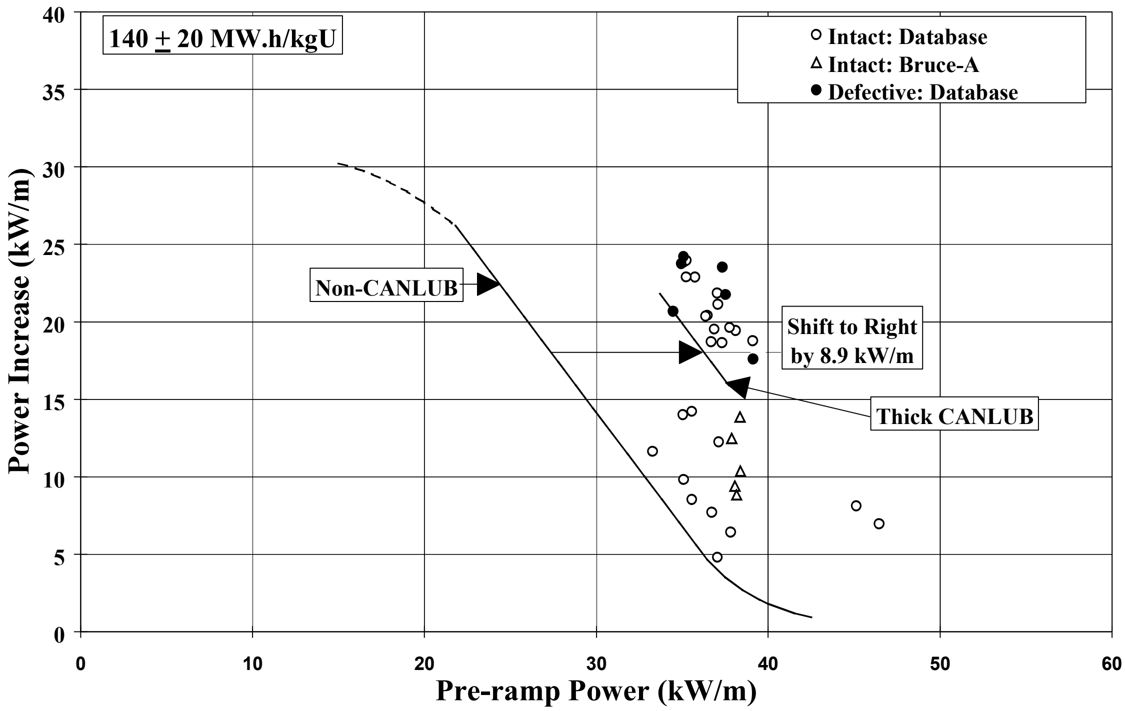

(a) Effect of CANLUB: 140 ± 20 MW•h/kgU

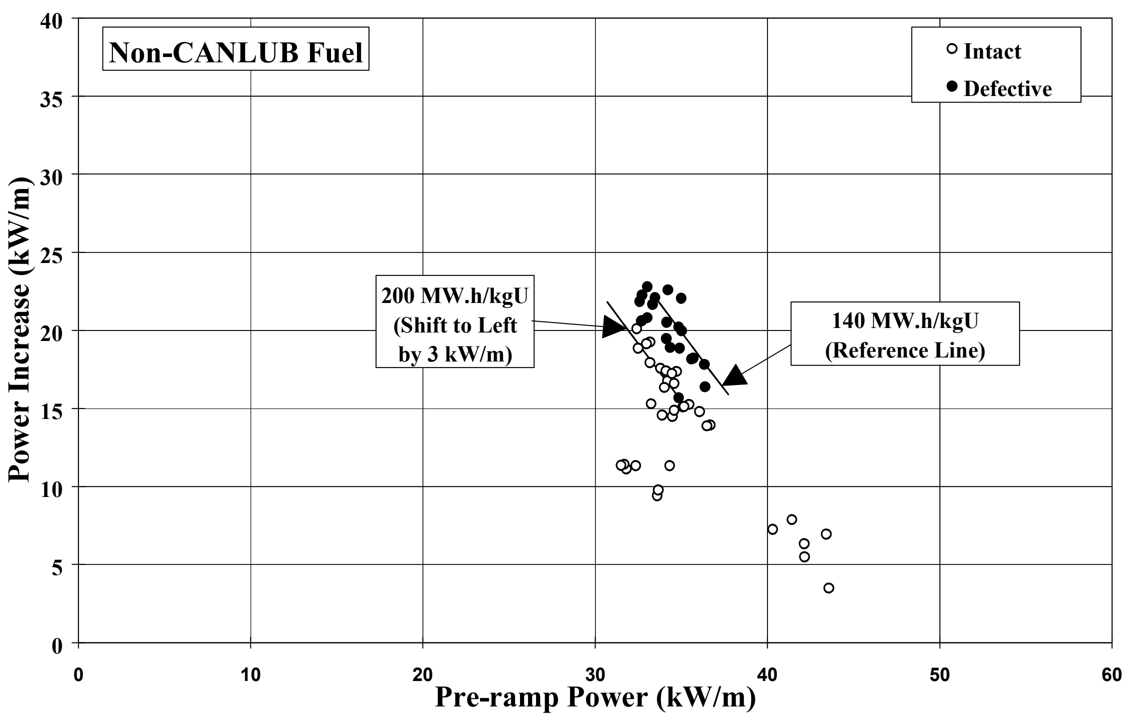

(b) Effect of Burnup: non-CANLUB fuel at 200 ± 20 MW•h/kgU

Figure 4 Effects of Burnup and Thick CANLUB

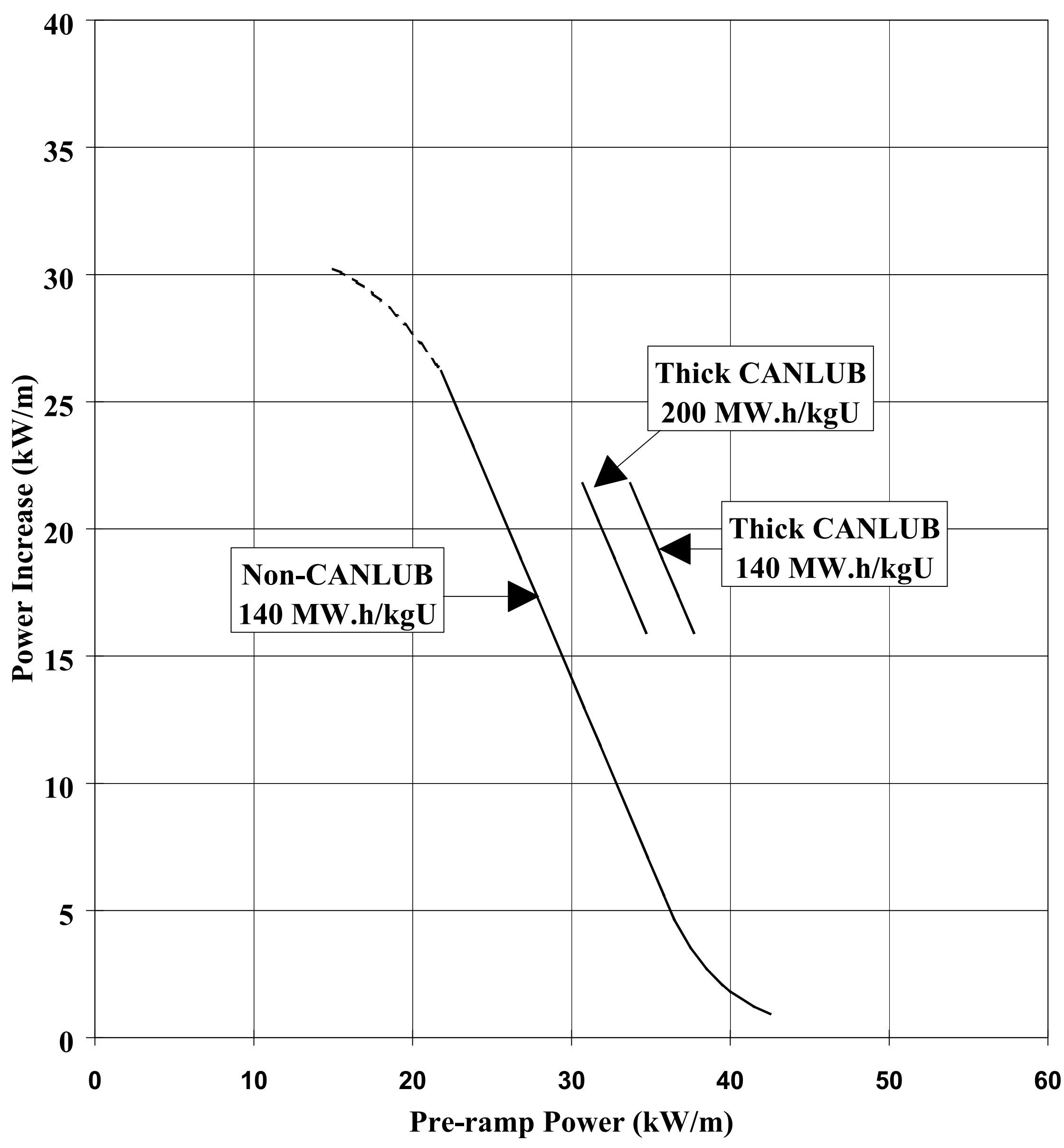

Figure 5 **Failure Thresholds**

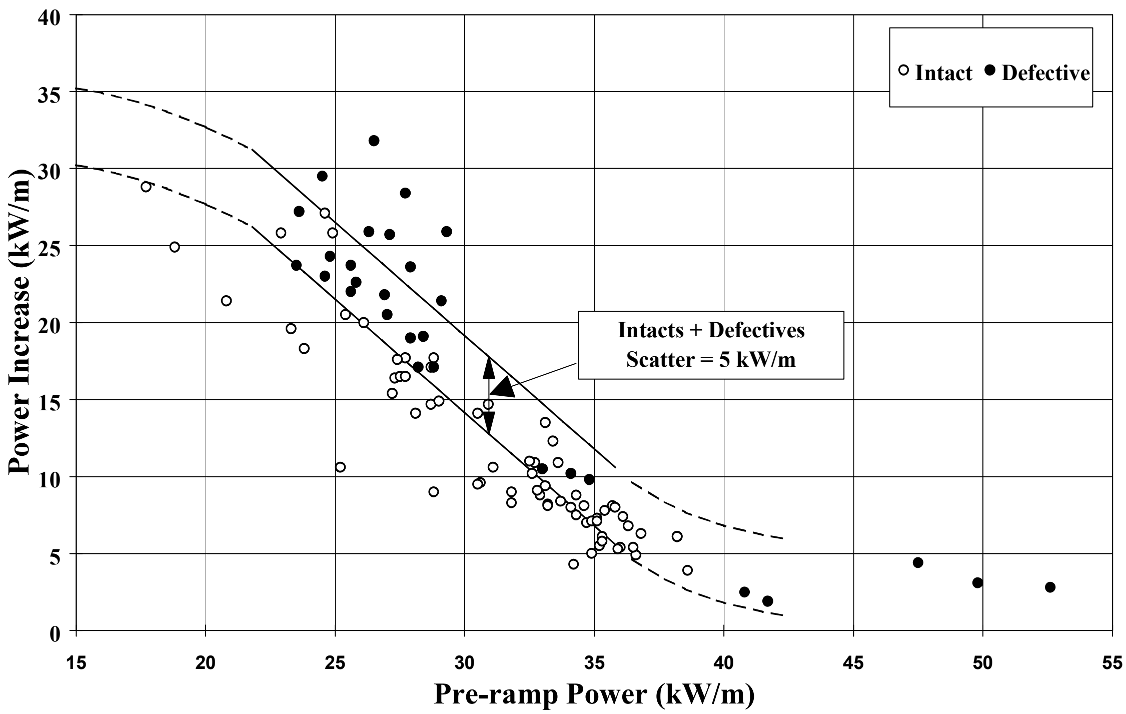

Figure 6 **Scatter in Data**

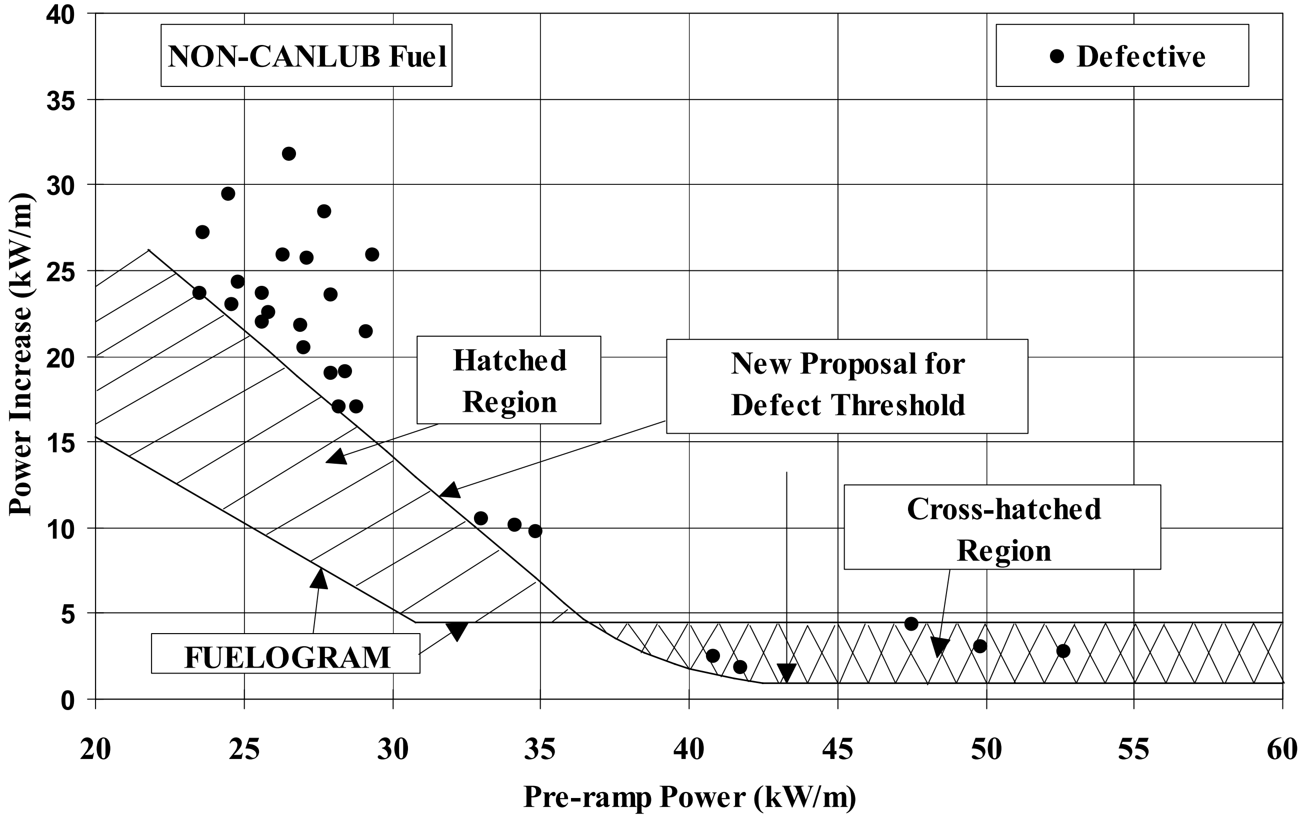

Figure 7 **Power-ramp Failed Fuel at 140 ± 20 MW•h/kgU**

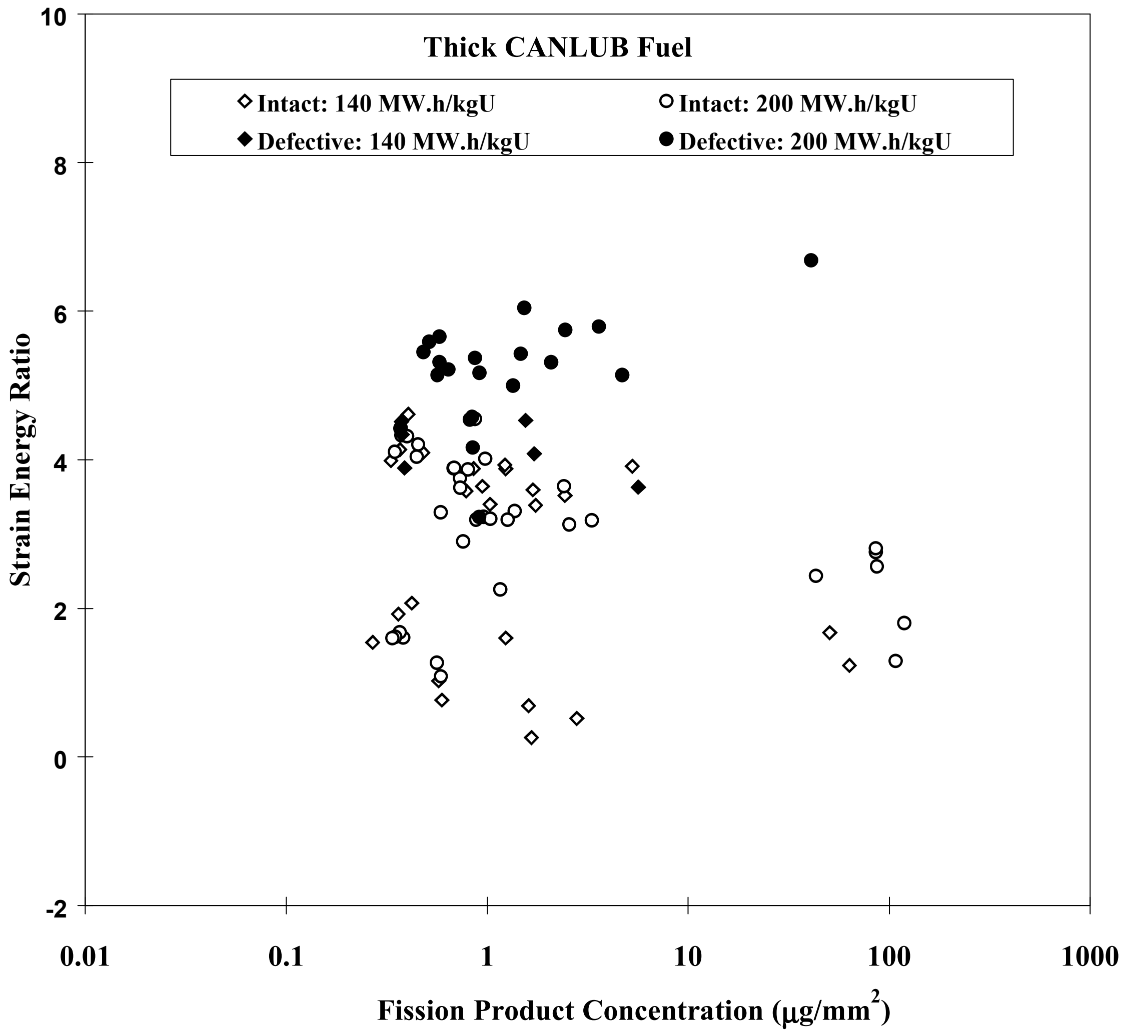

Figure 8 **Collapse of Data for Two Burnup-Ranges into One Family**